ACS Chemical Neuroscience

Research Article

pubs.acs.org/chemneuro

Discovery and Preclinical Validation of [^{11}C]AZ13153556, a Novel Probe for the Histamine Type 3 Receptor

Magnus Schou,*[,†] Katarina Varnäs,[‡] Anders Jureus,[§] Charlotte Ahlgren,[§] Jonas Malmquist,[§] Jenny Häggkvist,[‡] Lenke Tari,[‡] Steven S. Wesolowski,[∥] Scott R. Throner,[⊥] Dean G. Brown,[⊥] Maria Nilsson,[§] Peter Johnström,[†] Sjoerd J. Finnema,[‡] Ryuji Nakao,[‡] Nahid Amini,[‡] Akihiro Takano,[‡] and Lars Farde[†]

[†]AstraZeneca Translational Science Centre at Karolinska Institutet, PET Centre of Excellence, Department of Clinical Neuroscience, S-17176 Stockholm, Sweden

[‡]Department of Clinical Neuroscience, Psychiatry Section, Karolinska Institutet, S-17176 Stockholm, Sweden

[§]AstraZeneca, Research & Development, Innovative Medicines, S-151 85 Södertälje, Sweden

[∥]AstraZeneca, Research & Development, Innovative Medicines, Cambridge, Massachusetts 02451, United States

[⊥]AstraZeneca, Research & Development, Innovative Medicines, Waltham, Massachusetts 02139, United States

Supporting Information

ABSTRACT: The histamine type 3 receptor (H_3) is a G protein-coupled receptor implicated in several disorders of the central nervous system. Herein, we describe the radiolabeling and preclinical evaluation of a candidate radioligand for the H_3 receptor, 4-(1*S*,2*S*)-2-(4-cyclobutylpiperazine-1-carbonyl)-cyclopropyl]-*N*-methyl-benzamide (**5**), and its comparison with one of the frontrunner radioligands for H_3 imaging, namely, GSK189254 (**1**). Compounds **1** and **5** were radiolabeled with tritium and carbon-11 for in vitro and in vivo imaging experiments. The in vitro binding of [^{3}H]**1** and [^{3}H]**5** was examined by (i) saturation binding to rat and nonhuman primate brain tissue homogenate and (ii) in vitro autoradiography on tissue sections from rat, guinea pig, and human brain. The in vivo binding of [^{11}C]**1** and [^{11}C]**5** was examined by PET imaging in mice and nonhuman primates. B_{max} values obtained from Scatchard analysis of [^{3}H]**1** and [^{3}H]**5** binding were in good agreement. Autoradiography with [^{3}H]**5** on rat, guinea pig, and human brain slices showed specific binding in regions known to be enhanced in H_3 receptors, a high degree of colocalization with [^{3}H]**1**, and virtually negligible nonspecific binding in tissue. PET measurements in mice and nonhuman primates demonstrated that [^{11}C]**5** binds specifically and reversibly to H_3 receptors in vivo with low nonspecific binding in brain tissue. Whereas [^{11}C]**1** showed similar binding characteristics in vivo, the binding kinetics appeared faster for [^{11}C]**5** than for [^{11}C]**1**. Conclusions: [^{11}C]**5** has suitable properties for quantification of H_3 receptors in nonhuman primate brain and has the potential to offer improved binding kinetics in man compared to [^{11}C]**1**.

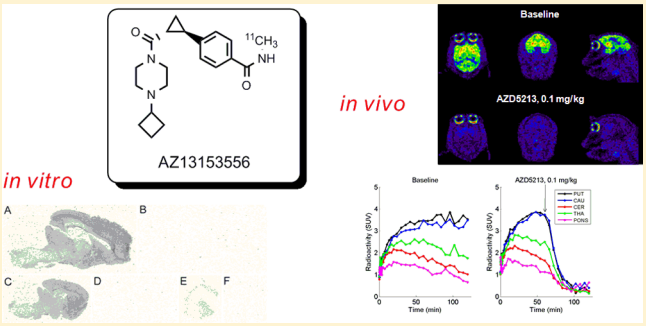

KEYWORDS: *PET, radioligand, receptor, imaging, histamine, carbon-11*

1. INTRODUCTION

Histamine, despite its simple chemical structure, is involved in many aspects of human physiology. In the central nervous system, histamine acts as a neurotransmitter, for which four receptor subtypes have been identified. Of these subtypes, the histamine type-3 (H_3) receptor has been suggested as a target for drug development based on reports implicating this receptor in the pathophysiology of neuropathic pain as well as cognitive disorders such as Alzheimer's disease (AD), Gilles de la Tourettes syndrome and schizophrenia.[1−5] The H_3 receptor is expressed primarily in the central nervous system (CNS) and only to a low extent in the periphery.[6]

The availability of a suitable positron emission tomography (PET) radioligand would be a valuable research tool to increase our understanding of H_3 receptor density and function in relation to the pathophysiology of CNS disorders. In addition, a PET radioligand may play a key role in the rational progression of a drug candidate through the establishment of target engagement and target occupancy.

Several H_3 PET radioligands have indeed been reported,[7−12] of which GSK189254 (**1**, Figure 1), two *spiro*-isobenzofuranone

Received: October 9, 2015
Accepted: November 3, 2015
Published: November 3, 2015

DOI: 10.1021/acschemneuro.5b00268
ACS Chem. Neurosci. 2016, 7, 177−184

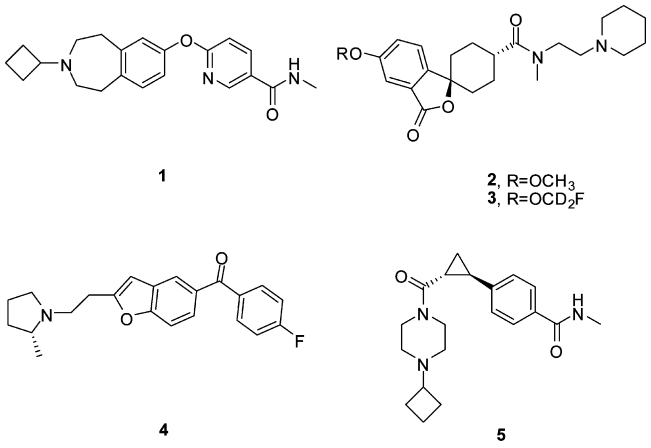

Figure 1. Structures of some PET radioligands for the H_3 receptor subtype. Compounds **1** and **5** are also known as GSK189254 and AZ13153556, respectively.

ligands (**2**, **3**), and the 2-aminoethylbenzofuran ligand (**4**) have shown saturable binding in vivo.[9,11,12] Of these, [^{11}C]**1** has been successfully applied in human subjects for examining drug induced receptor occupancy.[13] However, the binding kinetics of this compound are slow in regions with high H_3 density, (e.g., striatum), leading to high variance in estimates of binding parameters.[13] The use of [^{11}C]**1** should therefore mainly be restricted to regions having a low density of H_3 receptors, such as the neocortex. Moreover, **1** has subnanomolar affinity for the H_3 receptor, and by consequence there are stringent requirements on its specific radioactivity, since even low masses of **1** have shown reduction of specific binding to the H_3 receptor in a clinical trial with the radioligand (ED_{50} = 0.003 μg/kg).[13]

In search for an improved H_3 radioligand with more suitable binding kinetics, compounds with a lower H_3 affinity than **1** would be of primary interest. A diverse set of H_3 antagonists were available at AstraZeneca due to a long-standing interest in this target. Among these, **5** was identified as a potential novel PET radioligand for H_3. The affinity of **5** was roughly four times lower than that observed with **1** in a preliminary pharmacological assay (AstraZeneca, data on file). The compound has negligible affinity for the H_1 and H_4 receptors (>20 μM), low lipophilicity (log $D_{7.4}$ 1.73), and a chemical structure allowing facile radiolabeling via radiomethylation. In addition, **5** is an analogue of AZD5213, a candidate drug with demonstrated brain exposure in clinical trials.[14]

The aim of the present study was to perform a preclinical assessment of **5** as a candidate PET radioligand for human H_3 imaging. In addition, to the best of our knowledge, the first nonhuman primate PET studies with [^{11}C]**1** were conducted herein to enable a head-to-head comparison with [^{11}C]**5**.

2. RESULTS AND DISCUSSION

2.1. Radiochemistry. To enable an in vitro and in vivo comparison of the candidate radioligand **5** with comparator **1**, we first set out to radiolabel the compounds with tritium and carbon-11. For the preparation of [^{3}H]**1** and [^{11}C]**1**, only minor modifications were made to the reported procedure.[11] For the preparation of tritiated and carbon-11 labeled **5**, [^{3}H]methyl nosylate and [^{11}C]methyl iodide were used to introduce the radiolabel under alkaline conditions, respectively (Scheme 1). In terms of reaction rates, the tritiation reaction was completed within 1 h whereas the ^{11}C-radiolabeling reaction did not require

Scheme 1. Preparation of [^{3}H]5 ([^{3}H]Methyl Nosylate, NaH, DMF) and [^{11}C]5 ([^{11}C]Methyl Iodide, KOH, DMSO)[a]

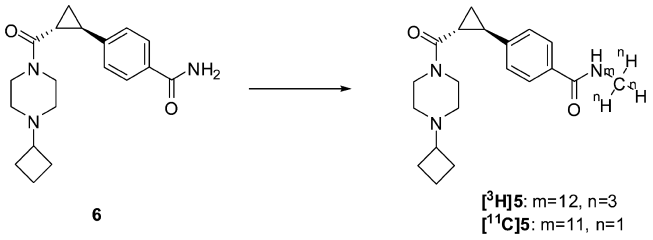

[a]The reaction was carried out at ambient temperature.

additional reaction time than that required to complete the entrapment of [^{11}C]methyl iodide (about 1 min). [^{3}H]**5** was isolated as the citrate salt with a specific radioactivity of 3.1 TBq/mmol and >99.9% radiochemical purity and its isotopologue, [^{11}C]**5**, was obtained at a specific radioactivity >111 GBq/μmol and a radiochemical purity exceeding 95%. The crude radiochemical yield of [^{11}C]**5** was 75% from [^{11}C]methyl iodide and the uncorrected radiochemical yield was 4% based on the estimated amount of cyclotron produced [^{11}C]CH_4.

The process, although not optimized, is expected to produce [^{11}C]**5** in sufficient amount and quality for clinical studies without major modifications.

2.2. In Vitro Saturation Analysis. The binding of [^{3}H]**1** and [^{3}H]**5** to rodent and NHP brain homogenate was saturable and could be described by a single site model. Scatchard analysis demonstrated a consistent B_{max} between the two ligands as well as a 3-fold lower K_D for **5** compared to **1** (Table 1). In agreement

Table 1. Dissociation Constants and Target Protein Concentrations in Membranes from the Frontal Cortex of Rodents and Striatum of Nonhuman Primates

	rat		NHP	
	K_D (nM)	B_{max} (fmol/mg wet tissue)	K_D (nM)	B_{max} (fmol/mg wet tissue)
[^{3}H]**1**	1.0	8.1	0.1	4.8
[^{3}H]**5**	3.0	10.5	0.3	4.4

with previous reports on H_3 receptor ligands there was a considerable interspecies difference in the binding affinity of **5** in NHP compared to rat brain tissue, with the molecule being roughly 10-fold more potent at the NHP isoform of the receptor. The relatively lower affinity of **1** to the rat H_3 receptor observed in our study is consistent with the previously observed 6-fold higher K_D of **1** in human brain reported by Medhurst et al.[15]

B_{max} and K_D are important variables in candidate radioligand selection through their relationship with the binding potential (BP = B_{max}/K_d), which is one of the main outcome parameters from a brain PET study. To assess the suitability of **5** as a PET radioligand candidate, BP was calculated from the B_{max} and K_d determined in vitro. Gratifyingly, the in vitro BP for **5** was 15 in NHP striatum, which is in the range of other successful CNS PET radioligands.[16] Furthermore, the high fraction target bound of **5** (>0.9), a parameter also taking the nonspecific binding of a ligand into account,[17] provided additional confidence for progressing [^{11}C]**5** as a radioligand candidate for in vivo imaging of the H_3 receptor.

2.3. In Vitro Autoradiography. The regional distribution of [^{3}H]**5** (Figure 2) was similar between rat and guinea pig and in agreement with H_3 mRNA and receptor distribution in the

DOI: 10.1021/acschemneuro.5b00268
ACS Chem. Neurosci. 2016, 7, 177−184

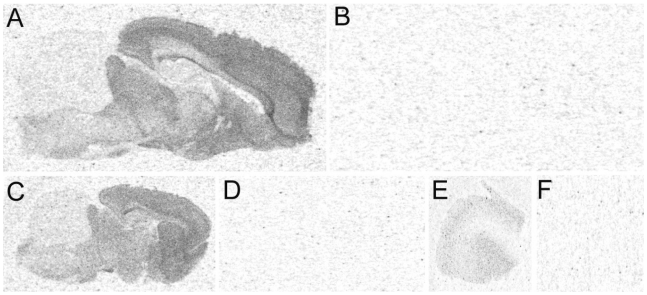

Figure 2. Binding distribution of 10 nM of [^{3}H]**5** to sagital sections from (A) guinea pig, (C) rat, and (E) human AD prefrontal cortex. Images (B), D), and (F) show nonspecific binding determined in the presence of 10 μM unlabeled **1**.

rodent brain.[18] In addition, its distribution pattern shared characteristics with other radioligands for in vitro H_3 imaging, such as [^{3}H]A-349821 and [^{3}H]**1**.[19,20] High levels of specific binding were thus observed in cortex and different parts of basal ganglia such as caudate putamen, nucleus accumbens, and globus pallidus, but also in parts of thalamus and hypothalamus. Low levels of binding were found in hippocampus, mostly associated with the CA1 area but also in dentate gyrus. Furthermore, specific binding could be detected in gray-matter regions of prefrontal cortex from an Alzheimer's disease patient, demonstrating cross-reactivity to human brain. Virtually all binding to rat, guinea pig and human brain could be displaced with 10 μM of **1**, thus supporting the view that **1** and **5** share the same binding site at the H_3 receptor as well as demonstrating the low nonspecific binding of [^{3}H]**5**.

2.4. PET. As described in the following, we found that [^{11}C]**5** satisifies several of the requirements of a suitable PET radioligand for central neuroreceptor imaging in vivo, namely: (i) adequate brain exposure for brain imaging, (ii) regional brain distribution in accordance with receptor localization, and (iii) saturable and reversible binding to the target protein.

2.4.1. Adequate Brain Exposure for Brain Imaging. Following intravenous injection of [^{11}C]**5**, radioactivity entered brain to a greater extent in nonhuman primates than in mice (Figures 3 and 4). At the time of C_{max} in monkeys (36−54 min post injection, Figure 4A), 2.2−2.7% (n = 3) of the injected radioactivity was present in brain. This peak in radioactivity was followed by a slow wash-out from brain during remaining time of the PET measurement. In three of four baseline PET measurements with [^{11}C]**1**, brain radioactivity only approached a peak toward 120 min of PET data acquisition and the C_{max}, 5.2−6.5% of the injected radioactivity (n = 3; Figure 4B), was observed at the end of the PET measurement.

2.4.2. Regional Brain Distribution in Accordance with Receptor Expression. Following injection of [^{11}C]**5**, the regional distribution of radioactivity in brain was heterogeneous. In mice, the highest concentration of radioactivity was found in the striatum and cortex, whereas cerebellum with its low brain uptake was identified as a candidate reference region (Figure 3A).

In monkey, the following rank order in regional radioactivity concentration was obtained: striatum > cerebellum ~ thalamus ~ cortex > pons (candidate reference region) (Figure 4C). The corresponding regional monkey brain distribution after intravenous injection of [^{11}C]**1** showed a similar pattern as that observed for [^{11}C]**5** (Figure 4D).

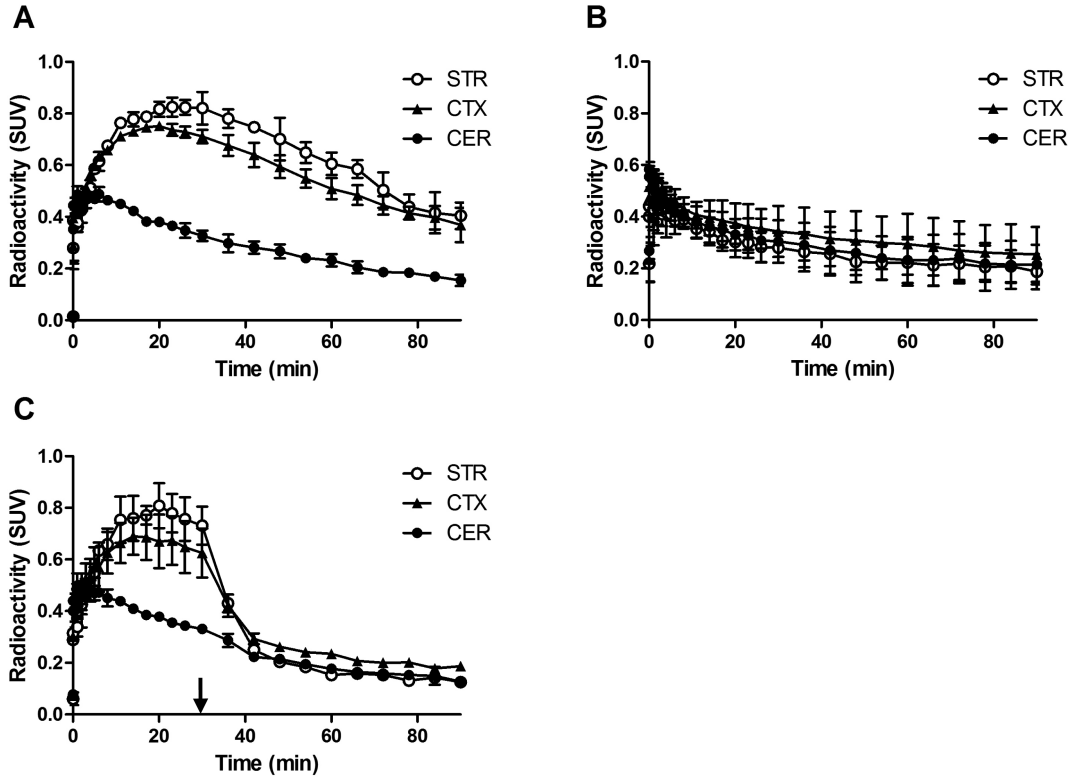

Figure 3. Time curves for the concentration of radioactivity in various mouse brain regions as a function of time following intravenous injection of [^{11}C]**5** under baseline (A), pretreatement (B), and displacement conditions (AZD5213, 1 mg/kg) (C). The arrow indicates the start of the displacement experiment. STR, striatum; CTX, cortex; CER, cerebellum.

DOI: 10.1021/acschemneuro.5b00268
ACS Chem. Neurosci. 2016, 7, 177−184

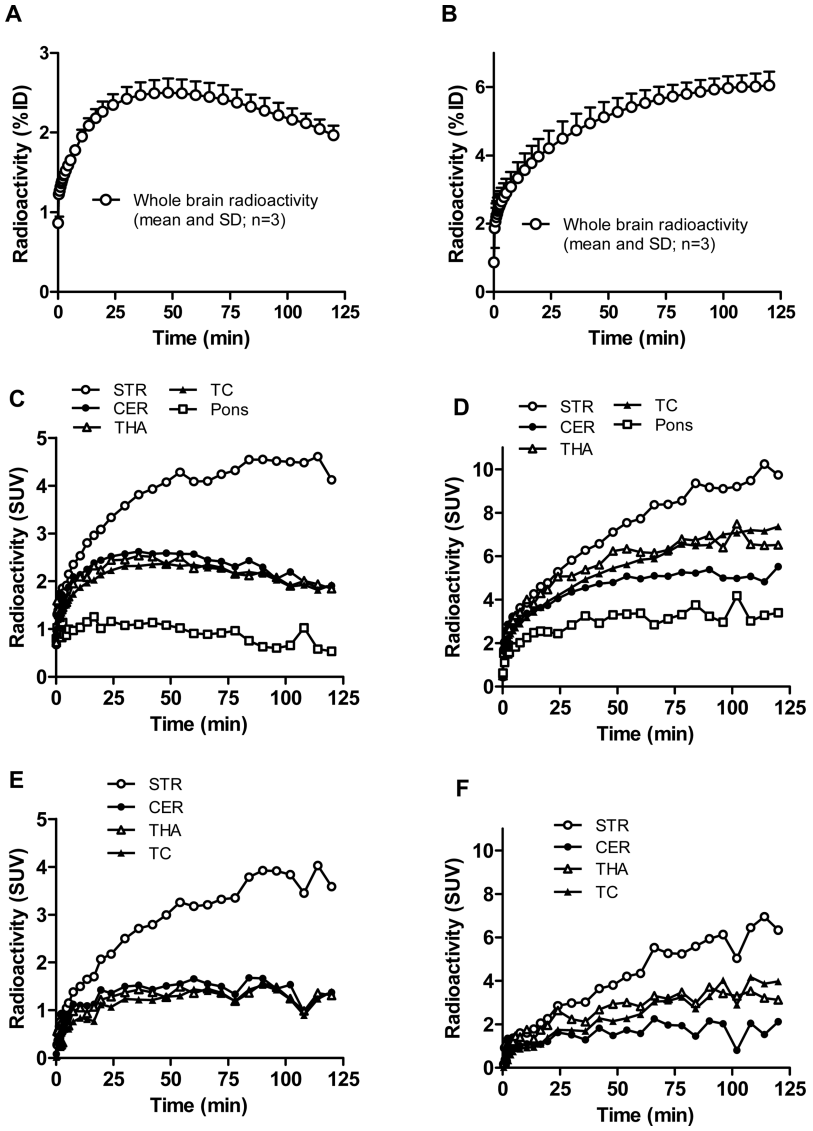

Figure 4. Brain radioactivity after injection of [^{11}C]**1** (A, C, E) and [^{11}C]**5** (B, D, F) in cynomolgus and rhesus monkeys. (A, D) Mean (SD) whole brain radioactivity in three monkeys expressed as percentage of injected radioactivity. (B, E) Regional radioactivity in monkey brain. (C, F) Radioactivity representing specific binding estimated as the difference between radioactivity in regions of interest and in a reference region (pons). STR, striatum; CER, cerebellum; THA, thalamus; TC, temporal cortex.

2.4.3. Saturable and Reversible Binding to the Target Protein. The primary reason for selecting **5** as a radioligand candidate, apart from its suitable physicochemical properties, was that its relatively lower affinity in a preliminary pharmacological assay implied that more rapid binding kinetics could be obtained with [^{11}C]**5** than with [^{11}C]**1**. Indeed, peak specific binding was obtained with [^{11}C]**5** in mice at about 30 min post injection in both striatum and cortex (Figure 3A). In monkeys, with the possible exception for the striatum, curves for specific [^{11}C]**5** binding also peaked within time of PET data acquisition (Figure 4E). For the reference radioligand [^{11}C]**1**, the corresponding curves for regional specific binding showed a trend of increasing binding with time throughout the PET examination (Figure 4F). The more rapid binding kinetics observed with [^{11}C]**5** may, at least in part, be explained by the 3-fold lower affinity of [^{11}C]**5** for the H_3 receptor in vitro.

In pretreatment experiments with the selective H_3 antagonist AZD5213 in a dose known to induce >95% occupancy at the H_3 receptor in the human brain,[14] the specific binding of [^{11}C]**5** was abolished and a uniform distribution of radioactivity was observed in brain (Figure 3B, 5, Figure 6B). A similar marked inhibition of specific binding was also observed when AZD5213 was administered before [^{11}C]**1** (data not shown). In a pretreatment experiment using the reference ligand ciproxifan, however, specific [^{11}C]**5** binding was only partially reduced (Figure 6C and D). It is likely that the partial reduction of [^{11}C]**5** binding is due to an incomplete blockade of H_3 receptors at the present conditions, since a similar partial reduction in binding was observed by Bao et al. for [^{18}F]**4** when using the same dose of ciproxifan (2.0 mg/kg).[12]

In the next series of experiments, specific [^{11}C]**5** binding was further characterized by a displacement experiment in which AZD5213 was administered after injection of [^{11}C]**5**. Following injection of AZD5213, there was a rapid reduction of [^{11}C]**5** binding in all brain regions (Figures 3C and 7B), demonstrating the rapid reversibility of [^{11}C]**5** binding to the H_3 receptor.

2.4.4. Kinetic Modeling. To examine the validity of pons as a reference region, we performed a preliminary pharmacokinetic

DOI: 10.1021/acschemneuro.5b00268
ACS Chem. Neurosci. 2016, 7, 177−184

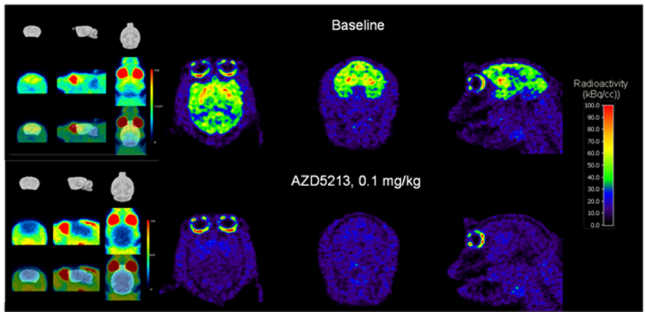

Figure 5. Representative color coded PET images showing distribution of radioactivity in mouse (left) and cynomolgus monkey (right) brain following intravenous injection of [^{11}C]**5** under baseline (top) and pretreatment conditions (AZD5213, 0.1 mg/kg; bottom). The images represent a summation of radioactivity from 9 to 93 min after [^{11}C]**5** injection. Image intensity was corrected for injected radioactivity.

modeling of the PET data obtained for a rhesus monkey at baseline and after administration of AZD5213. Time−activity curves derived from the baseline measurement could be described with both the 1-tissue compartment (TC) and 2-TC models showing no statistical preference for either of the models, whereas for the pretreatment measurement the 2-TC model was statistically preferred over the 1-TC model. Following pretreatment with AZD5213, a 33% reduction in the total distribution volume (V_T) for pons was observed compared to the corresponding baseline V_T value (Table 2). Thus, [^{11}C]**5** shows non-negligible specific binding in pons, which disqualifies this brain region as a suitable reference region in PET studies of the H_3 receptor in NHP. Arterial blood sampling is thus required

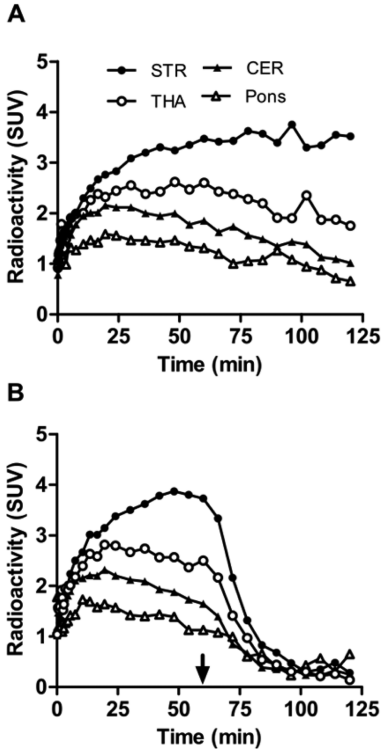

Figure 7. Time curves for the concentration of radioactivity in various brain regions as a function of time following intravenous injection of [^{11}C]**5** under baseline (A) and displacement conditions (AZD5213, 0.1 mg/kg) (B). The arrow indicates the start of the displacement experiment. STR, striatum; THA, thalamus; CER, cerebellum.

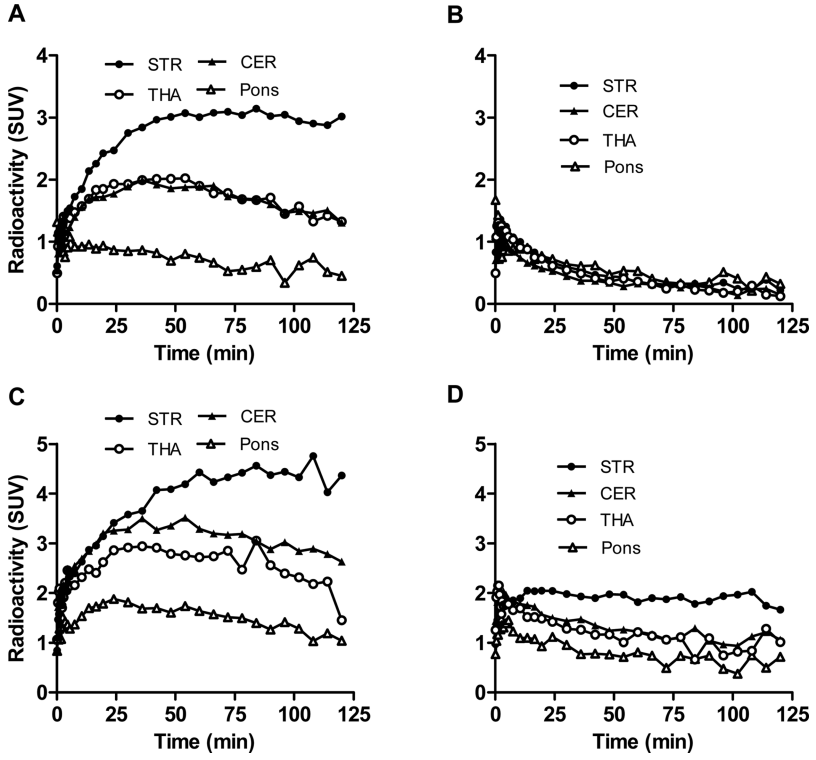

Figure 6. Time curves for the concentration of radioactivity in various brain regions as a function of time following intravenous injection of [^{11}C]**5** at baseline (A, C) and pretreatment conditions with AZD5213 (0.1 mg/kg) (B) and ciproxifan (2.0 mg/kg) (D). STR, striatum; THA, thalamus; CER, cerebellum.

DOI: 10.1021/acschemneuro.5b00268
ACS Chem. Neurosci. 2016, 7, 177−184

Table 2. Total Distribution Volume, Estimated Using the 2-Tissue Compartment Model, at Baseline and after Pretreatment with AZD5213

brain region	$V_{T,\ baseline}$	$V_{T,\ AZD5213}$
caudate nucleus	20	1.4
putamen	18	1.3
cerebellum	7.1	1.1
thalamus	6.9	1.2
pons	2.1	1.4

in future PET studies using [^{11}C]**5** for the quantitative analysis of H_3 receptors in the NHP brain.

2.4.5. Radioligand Metabolism. The time-course for metabolism of [^{11}C]**5** was followed in arterial and venous monkey plasma. At 4 and 90 min post injection, 86 ± 1% and 37 ± 6% (n = 5) of the radioactivity corresponded to [^{11}C]**5**, respectively. Two major radiometabolites of [^{11}C]**5** were observed (M1 and M2), with retention times of 2.2 and 4.3 min, respectively (Figure 8). These radiometabolites eluted

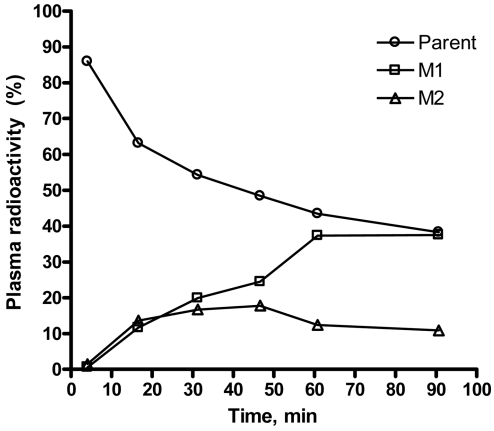

Figure 8. Time-course for parent radioligand and major radiometabolites in plasma.

before [^{11}C]**5** (t_R = 6.5 min) in the employed analytical HPLC method and may thus be considered as more polar than the parent compound. Further work will be conducted to understand the contribution of these polar radiometabolites to the brain PET images, if any. The free fraction of [^{11}C]**5** in plasma was 83%.

At 4 and 90 min post injection, 99% and 24% of the radioactivity corresponded to [^{11}C]**1**, respectively. The free fraction of [^{11}C]**1** in plasma was 54%.

3. CONCLUSIONS

[^{11}C]**5** has suitable preclinical characteristics for imaging H_3 receptors in the NHP brain with PET. In addition, the present study suggests that [^{11}C]**5** has more rapid binding kinetics in brain than [^{11}C]**1**, although there is still some room for improvement with regard to the binding kinetics in regions having a high H_3 receptor density.

4. METHODS

4.1. Radiochemistry. HPLC solvents were obtained from Fisher (Sweden). All other reagents and solvents, including anhydrous solvents, were obtained from Sigma-Aldrich (Sweden) and used without further purification.

4.1.1. Tritium Labeling. [^{3}H]methyl nosylate was purchased from RC TRITEC AG, Teufen. Mass spectra were recorded on a Waters LCMS consisting of a Waters 1525 micro (LC), Waters PDA 2996, and ELS detector (Sedex 75) and a ZMD single quadrupole mass spectrometer. Tritium HPLC analyses were performed on a Agilent 1100, HPLC system with a binary pump, autoinjector, DAD and column oven, coupled in series with a Packard Radiomatic Flow Scintillator 525TR, equipped with a solid scintillator (SolarScint) cell with a volume of 33 μL. A Gemini column (C18, 3 × 100 mm, 5 μm) was used with the column temperature set to 40 °C using a gradient of 5−95% acetonitrile in 10 mM ammonium acetate in Milli-Q water at 1 mL/min over 13.5 min. Purities were reported as UV area% or radioactive area% by HPLC. Preparative chromatography was run on a Kromasil column (C8, 5 μm, 10 × 250 mm) using 35% acetonitrile/50 mM ammonium acetate in Milli-Q Water at 2 mL/min. Liquid scintillation analysis was performed on a Packard Tricarb 2900TR.

*[^{3}H]**5***. 4-((1*S*,2*S*)-2-(4-Cyclobutylpiperazine-1-carbonyl)-cyclopropyl)benzamide **6** (1 mg, 3.0 μmol) was dissolved in *N*,*N*-dimethylformamide (1 mL), and sodium hydride (0.28 mg, 0.01 mmol) was added. [^{3}H]Methyl 4-nitrobenzenesulfonate (518 MBq, >2.2 TBq/mmol) was added. The mixture was stirred at ambient temperature for approximately 1 h. The reaction was quenched with ammonium chloride (sat., 0.5 mL). The mixture was extracted with ethyl acetate (1 mL) thrice. The organic phase was dried over sodium sulfate, was filtered, and was concentrated with respect to ethyl acetate. The remaining solution was purified by HPLC on the Kromasil system. The pooled fractions were concentrated and was dissolved in ethanol (70%, 3.38 mL), and citric acid (0.2 mg, 1.0 μmol) was added to give [^{3}H]-4-((1*S*,2*S*)-2-(4-cyclobutylpiperazine-1-carbonyl)cyclopropyl)-*N*-methylbenzamide citrate [^{3}H]**5** (53 MBq, 3.1 TBq/mmol) at a 100% radiochemical purity. The product coeluted with cold material. LC-MS m/z 346.2 (5%), 348.2 (100%) ([M + H]$^+$).

4.1.2. Carbon-11 Labeling. [^{11}C]Methane was produced using 16 MeV protons in the ^{14}N(p,α)^{11}C reaction on a mixture of nitrogen and hydrogen gas (10% hydrogen). [^{11}C]Methane was isolated from the target gas and subsequently converted into [^{11}C]methyl iodide by radical iodination of [^{11}C]methane in a recirculation system as previously described elsewhere.[21] Radiomethylation, purification, and formulation was performed using a computer controlled automated system (Scansys, Denmark). Semipreparative HPLC was performed using a reverse phase μ-Bondapak C-18 column (300 × 7.8 mm, 10 μm; Waters) eluted with MeCN-NH_4OAc (50 mM, pH 4.7), 15:85 v/v at 6 mL/min. The column outlet was connected with an absorbance detector (λ = 254 nm) in series with a radiation detector. The retention time of **5** was 8 min in this system. The radiochemical purity of **5** was determined by reverse phase HPLC using a μ-Bondapak C-18 column (300 × 3.9 mm, 10 μm; Waters) and an absorbance detector (λ = 254) in series with a β-flow detector (Beckman) for radiation detection. The HPLC column was eluted with MeCN−H_3PO_4 (10 mM), 10:90 v/v at 3 mL/min. The retention time of **5** was 5.0 min in this system. Specific radioactivity for **5** was determined by HPLC using a μ-Bondapak C-18 column (300 × 3.9 mm, 10 μm; Waters) eluted with MeCN-HCO_2NH_4 (50 mM), 15:85 v/v at 2 mL/min. The retention time of **5** was 21.8 min in this system. [^{11}C]**1** was produced according to the previously described method.[2] Preparative and analytical chromatograms can be found in the Supporting Information.

*[^{11}C]**5***. [^{11}C]Methyl iodide was trapped in a well-agitated suspension of **6** (0.5 mg, 2 μmol) and potassium hydroxide (5 mg, 89 μmol) in DMSO (400 μL). After completed entrapment, the crude reaction mixture was diluted with NH_4OAc (50 mM, 600 μL) and purified by HPLC. The fraction containing the title compound was evaporated to dryness and redissolved in a solution of ethanol (5% v/v) in physiologically buffered saline (PBS) at pH 7.4 (6.5 mL). The solution was sterilized by membrane filtration (0.22 μm yellow filter, Millipore) to yield the final product in a solution ready for injection. [^{11}C]**5** coeluted with an unlabeled reference standard of **5** on HPLC. Its identity was further confirmed by tandem mass spectrometry (MS/MS) analysis of the carrier associated with [^{11}C]AZ13153556 and comparison with an authentic reference standard.

4.2. In Vitro Saturation Analysis. [^{3}H]**5** saturation studies were carried out in duplicate with 20−50 μg protein/tube in 2 mL buffer consisting of 50 mM Tris-HCl, 4 mM MgCl2, 1 mM EDTA (pH 7.4 at

DOI: 10.1021/acschemneuro.5b00268
ACS Chem. Neurosci. 2016, 7, 177−184

30 °C), and 0.006−13 nM (11 concentrations) of radioligand. Nonspecific binding was defined with 10 μM unlabeled **1**. Receptor binding experiments were incubated for 2−3 h at 30 °C, and stopped by rapid filtration through Whatman GF/B glass fiber filters and subsequent washing with cold buffer (5 mM Tris-HCl, pH 7.4) using a Brandel cell harvester. Scintillation cocktail was added and the radioactivity determined in a Packard 2500TR liquid scintillation counter at about 50% efficiency.

4.3. In Vitro Receptor Autoradiography. In vitro autoradiography was performed on 10 μm thick cryo-cut tissue sections from rat guinea pig or human postmortem AD brain thaw-mounted onto microscope slides (SuperFrost Plus slides, Menzel GmbH, Braunschweig, Germany). The slides were preincubated in 50 mM Tris buffer (pH 7.4) containing 3 mM $MgCl_2$ at room temperature followed by 30 min incubation with [^{3}H]**5** in the Tris-$MgCl_2$ buffer. Finally, the sections were washed (3 × 10 min) in the same buffer at 1 °C followed by a rinse in deionized water (1 °C) and air-dried at room temperature in front of a fan. For competition studies, brain sections were coincubated for 30 min at room temperature in 50 mM Tris buffer (pH 7.4) with [^{3}H]**5** and competing ligand **1**. Radiolabeled sections and plastic tritium standards (Amersham, Pharmacia Biotech, Piscataway, NJ, USA) were exposed to phosphoimage (PI) plates (Fuji BAS-TR2040) for 10 days. Phosphoimage plates were processed with a Fujifilm FLA7000 phosphoimager (Fuji, Tokyo, Japan). Binding was analyzed with Multigauge software V3.0 (Fuji) using the relative optical density values generated from coexposed tritium standards.

4.4. Human Tissue. Cortical samples from AD patients were acquired from The Netherlands Brain Bank and used to examine the binding of test compounds to β-amyloid plaques. The tissue samples were used in accordance with the Swedish Biobank Law and AstraZeneca guidelines to protect the integrity of the donor.

4.5. PET in Mice. The experiments were performed in accordance with the guidelines of the Swedish National Board of Laboratory Animals under protocols approved by the Animal Ethics Review Board of Northern Stockholm, Sweden (Dnr N557/11). Male C57Bl6 mice (Charles River, Germany), were housed in groups in a temperature (±21 °C) and humidity (±40%) controlled environment on a 12 h light/dark cycle (lights on 7:00 AM) with ad libitum access to food and water. Two mice were imaged with [^{11}C]AZ13153556 on three different experimental session. The sessions were performed with a minimum of 1 week between each imaging session. Session 1: Baseline PET measurement (injected radioactivity (RA) 12 MBq and 12.5 MBq respectively). Session 2: Pretreatment PET measurement in which AZD5213 (1 mg/kg, i.v.) was given 28 min before injection of [^{11}C]AZ13153556 (injected RA 12 MBq and 12.6 MBq respectively). Session 3: displacement PET measurement in which AZD5213 (1 mg/kg, i.v.) was administered 30 min after injection of [^{11}C]AZ13153556 (injected RA 8.8 MBq and 8.4 MBq respectively). The PET measurements were performed with a nanoScan PET/MRI and a nanoScan PET/CT (Mediso Ltd, Hungary) system. The two animals were examined at the same time in the identical PET modules of the two PET systems. On the experimental day, the animal was anaesthetized with inhalation isoflurane (4−5% isoflurane in 100% oxygen). After induction of anesthesia, the isoflurane concentration was reduced to 1.5−2% (50/50 air/oxygen) and the animals were positioned in a dedicated mouse holder. A cannula was inserted in the tail vein through which the radioligand was administered and the radioactivity in brain was measured continuously for 93 min. Upon completion the imaging sessions, the animal returned to its cage. The acquired list mode data was reconstructed into 35 time frames (93 min PET measurement = 4 × 10 s, 4 × 20 s, 4 × 60 s, 7 × 180 s, 11 × 360 s). The image reconstruction was made with a fully three-dimensional maximum-likelihood expectation maximization algorithm (MLEM) with 20 iterations, without scatter and attenuation correction. The reconstructed dynamic PET images were coregistered to an inbuilt mice MRI template available in PMOD, which also incorporates volumes of interest (VOIs) sets (PMOD Technologies Ltd., Zurich). With the help of these VOI sets, decay corrected time activity curves (TAC) were generated. The regional brain uptake values were expressed as percent standard uptake value (%SUV), which normalizes for injected radioactivity and body weight. The binding potential (BP_{ND}) was calculated in PMOD with the simplified reference tissue model (SRTM) using cerebellum as a reference region.

4.6. PET in Monkeys. The study was approved by the Animal Ethics Committee of the Swedish Animal Welfare Agency (Dnr 145/08, 399/08, and 386/09) and was performed according to the "Guidelines for planning, conducting and documenting experimental research" (Dnr 4820/06-600) of the Karolinska Institutet, the "Guide for the Care and Use of Laboratory Animals",[22] the AstraZeneca bioethics policy, and the EU Directive 2010/63/EU. Six cynomolgus monkeys (weighing 4.1−7.8 kg) and one rhesus monkey (weighing 5.6 kg) were supplied by Astrid Fagraeus Laboratory of the Swedish Institute for Infectious Disease Control, Solna, Sweden.

Seven PET measurements were performed with [^{11}C]**5** in four different experimental sessions. Session 1: Baseline PET measurement with 163 MBq of [^{11}C]**5** in cynomolgus monkey 1 (weight 5.8 kg). Session 2: Baseline PET measurement with 155 Mbq of [^{11}C]**5** in cynomolgus monkey 2 (weight 5.9 kg) followed by a displacement PET measurement in which AZD5213 (0.1 mg/kg) was infused during 10 min starting 1 h after injection of [^{11}C]**5** (154 MBq). Session 3: Baseline PET measurement with 156 Mbq of [^{11}C]**5** in a rhesus monkey (weight 5.5 kg) followed by a pretreatment PET measurement in which AZD5213 (0.1 mg/kg) was infused during 10 min starting at 30 min before injection of [^{11}C]**5** (153 MBq). Session 4: Baseline PET measurement with 149 Mbq of [^{11}C]**5** in cynomolgus monkey 1 (weight 7.8 kg) followed by a pretreatment PET measurement in which ciproxifan (2 mg/kg) was infused during 20 min starting 30 min before injection of [^{11}C]**5** (153 MBq).

Four baseline PET measurements were performed with [^{11}C]**1** in four sessions. Session 1: Baseline PET measurement in cynomolgus monkey 4 (weight 4.1 kg) with 106 MBq of [^{11}C]**1**. Session 2: Baseline PET measurement in cynomolgus monkey 5 (weight 5.8 kg) with 104 MBq of [^{11}C]**1**. Session 3: Baseline PET measurement in cynomolgus monkey 5 (weight 5.6 kg) with 105 MBq of [^{11}C]**1**. Session 4: Baseline PET measurement in cynomolgus monkey 4 (weight 6 kg) with 104 MBq of [^{11}C]**1**.

Anesthesia was induced by intramuscular injection of ketamine hydrochloride (ca. 10 mg/kg) and maintained by the administration of a mixture of sevoflurane, oxygen, and medical air after endotracheal intubation. The monkey was observed continuously during the PET experimental days. Body temperature was maintained by Bair Hugger model 505 (Arizant Healthcare Inc., MN) and monitored using an esophageal thermometer. Heart and respiration rates were continuously monitored using a PC-VetGard (TM) system (http://www.vmedtech.com/wireless_monitor.htm). A head fixation system was used to secure a fixed position of the monkey's head throughout the PET measurements undertaken in each experimental session.[23]

In each PET measurement, a sterile physiological phosphate buffer (pH 7.4) solution containing radiotracer was injected as a bolus into a sural vein during 5 s with simultaneous start of PET data acquisition. Radioactivity in brain was measured continuously for 123 min according to a preprogrammed series of 34 frames.

■ ASSOCIATED CONTENT

Supporting Information

The Supporting Information is available free of charge on the ACS Publications website at DOI: 10.1021/acschemneuro.5b00268.

Preparative chromatogram from the purification of [^{11}C]**1**; analytical chromatogram of formulated [^{11}C]**1** co-injected with a solution of authentic **1**; preparative chromatogram from the purification of [^{11}C]**5**; analytical chromatogram of formulated [^{11}C]**5** co-injected with a solution of authentic **5** (PDF)

■ AUTHOR INFORMATION

Corresponding Author

*E-mail: magnus.schou@astrazeneca.com. Tel: +468 51775598.

DOI: 10.1021/acschemneuro.5b00268
ACS Chem. Neurosci. 2016, 7, 177−184

Author Contributions

M.S. planned the experiments, performed the PET chemistry and wrote up the paper together with L.F. A.T., S.F., and P.J., K.V. performed and analyzed the nhp PET experimenets. A.J. and M.N. performed and analyzed the autoradiography experiments. C.A. performed and analyzed the saturation binding. J.H. and L.T. performed and analyzed the mice PET experiments. S.S.W., S.R.T. and D.G.B. designed and prepared molecule 1. R.N. and N.A. performed and analyzed the metabolism experiments.

Notes

The authors declare no competing financial interest.

■ ACKNOWLEDGMENTS

We are grateful to Arsalan Amir, Guennadi Jogolev, Gudrun Nylén, Julio Gabriel, and all other members of the PET center at Karolinska Institutet.

■ REFERENCES

(1) Alguacil, L. F., and Perez-Garcia, C. (2003) Histamine H3 receptor: a potential drug target for the treatment of central nervous system disorders. *Curr. Drug Targets: CNS Neurol. Disord. 2*, 303−313.

(2) Leurs, R., Vollinga, R. C., and Timmerman, H. (1995) The medicinal chemistry and therapeutic potentials of ligands of the histamine H3 receptor. *Prog. Drug. Res. 45*, 107−165.

(3) Karagiannidis, I., Dehning, S., Sandor, P., Tarnok, Z., Rizzo, R., Wolanczyk, T., Madruga-Garrido, M., Hebebrand, J., Nothen, M. M., Lehmkuhl, G., Farkas, L., Nagy, P., Szymanska, U., Anastasiou, Z., Stathias, V., Androutsos, C., Tsironi, V., Koumoula, A., Barta, C., Zill, P., Mir, P., Muller, N., Barr, C., and Paschou, P. (2013) Support of the histaminergic hypothesis in Tourette Syndrome: association of the histamine decarboxylase gene in a large sample of families. *J. Med. Genet. 50*, 760−764.

(4) Fernandez, T. V., Sanders, S. J., Yurkiewicz, I. R., Ercan-Sencicek, A. G., Kim, Y. S., Fishman, D. O., Raubeson, M. J., Song, Y., Yasuno, K., Ho, W. S., Bilguvar, K., Glessner, J., Chu, S. H., Leckman, J. F., King, R. A., Gilbert, D. L., Heiman, G. A., Tischfield, J. A., Hoekstra, P. J., Devlin, B., Hakonarson, H., Mane, S. M., Gunel, M., and State, M. W. (2012) Rare copy number variants in tourette syndrome disrupt genes in histaminergic pathways and overlap with autism. *Biol. Psychiatry 71*, 392−402.

(5) Hough, L. B., and Rice, F. L. (2011) H3 receptors and pain modulation: peripheral, spinal, and brain interactions. *J. Pharmacol. Exp. Ther. 336*, 30−37.

(6) Lovenberg, T. W., Roland, B. L., Wilson, S. J., Jiang, X., Pyati, J., Huvar, A., Jackson, M. R., and Erlander, M. G. (1999) Cloning and functional expression of the human histamine H3 receptor. *Mol. Pharmacol. 55*, 1101−1107.

(7) Airaksinen, A. J., Jablonowski, J. A., van der Mey, M., Barbier, A. J., Klok, R. P., Verbeek, J., Schuit, R., Herscheid, J. D., Leysen, J. E., Carruthers, N. I., Lammertsma, A. A., and Windhorst, A. D. (2006) Radiosynthesis and biodistribution of a histamine H3 receptor antagonist 4-[3-(4-piperidin-1-yl-but-1-ynyl)-[^{11}C]benzyl]-morpholine: evaluation of a potential PET ligand. *Nucl. Med. Biol. 33*, 801−810.

(8) Funaki, Y., Sato, K., Kato, M., Ishikawa, Y., Iwata, R., and Yanai, K. (2007) Evaluation of the binding characteristics of [^{18}F]fluoroproxyfan in the rat brain for in vivo visualization of histamine H3 receptor. *Nucl. Med. Biol. 34*, 981−987.

(9) Hamill, T. G., Sato, N., Jitsuoka, M., Tokita, S., Sanabria, S., Eng, W., Ryan, C., Krause, S., Takenaga, N., Patel, S., Zeng, Z., Williams, D., Jr., Sur, C., Hargreaves, R., and Burns, H. D. (2009) Inverse agonist histamine H3 receptor PET tracers labelled with carbon-11 or fluorine-18. *Synapse 63*, 1122−1132.

(10) Windhorst, A. D., Timmerman, H., Klok, R. P., Menge, W. M., Leurs, R., and Herscheid, J. D. (1999) Evaluation of [^{18}F]VUF 5000 as a potential PET ligand for brain imaging of the histamine H3 receptor. *Bioorg. Med. Chem. 7*, 1761−1767.

(11) Plisson, C., Gunn, R. N., Cunningham, V. J., Bender, D., Salinas, C. A., Medhurst, A. D., Roberts, J. C., Laruelle, M., and Gee, A. D. (2009) ^{11}C-GSK189254: a selective radioligand for in vivo central nervous system imaging of histamine H3 receptors by PET. *J. Nucl. Med. 50*, 2064−2072.

(12) Bao, X., Lu, S., Liow, J. S., Zoghbi, S. S., Jenko, K. J., Clark, D. T., Gladding, R. L., Innis, R. B., and Pike, V. W. (2012) Radiosynthesis and evaluation of an ^{18}F-labeled positron emission tomography (PET) radioligand for brain histamine subtype-3 receptors based on a nonimidazole 2-aminoethylbenzofuran chemotype. *J. Med. Chem. 55*, 2406−2415.

(13) Ashworth, S., Rabiner, E. A., Gunn, R. N., Plisson, C., Wilson, A. A., Comley, R. A., Lai, R. Y., Gee, A. D., Laruelle, M., and Cunningham, V. J. (2010) Evaluation of ^{11}C-GSK189254 as a novel radioligand for the H3 receptor in humans using PET. *J. Nucl. Med. 51*, 1021−1029.

(14) Jucaite, A., Takano, A., Bostrom, E., Jostell, K. G., Stenkrona, P., Halldin, C., Segerdahl, M., and Nyberg, S. (2013) AZD5213: a novel histamine H3 receptor antagonist permitting high daytime and low nocturnal H3 receptor occupancy, a PET study in human subjects. *Int. J. Neuropsychopharmacol. 16*, 1231−1239.

(15) Medhurst, A. D., Atkins, A. R., Beresford, I. J., Brackenborough, K., Briggs, M. A., Calver, A. R., Cilia, J., Cluderay, J. E., Crook, B., Davis, J. B., Davis, R. K., Davis, R. P., et al. (2007) GSK189254, a novel H3 receptor antagonist that binds to histamine H3 receptors in Alzheimer's disease brain and improves cognitive performance in preclinical models. *J. Pharmacol. Exp. Ther.* No. 321, 1032−1045.

(16) Eckelman, W. C., and Mathis, C. A. (2006) Targeting proteins in vivo: in vitro guidelines. *Nucl. Med. Biol. 33*, 161−4.

(17) Fridén, M., Wennerberg, M., Antonsson, M., Sandberg-Ställ, M., Farde, L., and Schou, M. (2014) Identification of positron emission tomography (PET) tracer candidates by prediction of the target-bound fraction in the brain. *EJNMMI Res. 4*, 50.

(18) Pillot, C., Heron, A., Cochois, V., Tardivel-Lacombe, J., Ligneau, X., Schwartz, J. C., and Arrang, J. M. (2002) A detailed mapping of the histamine H3 receptor and its gene transcripts in rat brain. *Neuroscience 114*, 173−193.

(19) Miller, T. R., Milicic, I., Bauch, J., Du, J., Surber, B., Browman, K. E., Marsh, K., Cowart, M., Brioni, J. D., and Esbenshade, T. A. (2009) Use of the H3 receptor antagonist radioligand [3H]-A-349821 to reveal in vivo receptor occupancy of cognition enhancing H3 receptor antagonists. *Br. J. Pharmacol. 157*, 139−149.

(20) Medhurst, A. D., Roberts, J. C., Lee, J., Chen, C. P., Brown, S. H., Roman, S., and Lai, M. K. (2009) Characterization of histamine H3 receptors in Alzheimer's Disease brain and amyloid over-expressing TASTPM mice. *Br. J. Pharmacol. 157*, 130−138.

(21) Schou, M., Pike, V. W., Varrone, A., Gulyas, B., Farde, L., and Halldin, C. (2006) Synthesis and PET evaluation of (*R*)-[*S*-methyl-^{11}C]thionisoxetine, a candidate radioligand for imaging brain norepinephrine transporters. *J. Labelled Compd. Radiopharm. 49*, 1007−1019.

(22) Clark, J. D., Gebhart, G. F., Gonder, J. C., Keeling, M. E., and Kohn, D. F. (1997) Special Report: The 1996 Guide for the Care and Use of Laboratory Animals. *ILAR J. 38*, 41−48.

(23) Karlsson, P., Farde, L., Halldin, C., Swahn, C. G., Sedvall, G., Foged, C., Hansen, K. T., and Skrumsager, B. (1993) PET Examination of [C-11]NNC-687 and [C-11]NNC756 as New Radioligands for the D-1-Dopamine Receptor. *Psychopharmacol. 113*, 149−156.

DOI: 10.1021/acschemneuro.5b00268
ACS Chem. Neurosci. 2016, 7, 177−184